Available online at www.sciencedirect.com
SCIENCE DIRECT®
Bioorganic & Medicinal Chemistry 12 (2004) 6527–6537
Bioorganic & Medicinal Chemistry

A molecular docking study of estrogenically active compounds with 1,2-diarylethane and 1,2-diarylethene pharmacophores

Peter M. Kekenes-Huskey,[a,b] Ingo Muegge,[c] Moriz von Rauch,[d] Ronald Gust[d] and Ernst-Walter Knapp[a,*]

[a]*Institut für Chemie, Freie Universität Berlin, Takustrasse 6, D14195 Berlin, Germany*
[b]*Materials and Process Simulation Center, California Institute of Technology, Pasadena, CA 91125, USA*
[c]*Boehringer Ingelheim Pharmaceuticals, Inc., 900, Ridgebury Rd., Ridgefield, CT 06877-0368, USA*
[d]*Institut für Pharmazie, Freie Universität Berlin, Königin-Luise Str. 2-4, D14195 Berlin, Germany*

Received 27 April 2004; revised 8 September 2004; accepted 14 September 2004
Available online 22 October 2004

Abstract—Numerous selective estrogen receptor modulators (SERMs) have been synthesized and assayed in recent years. The focus of this study is to apply coarse-grain molecular docking procedures coupled with fine-grain all-atom force field optimization strategies to shed light on the binding mechanisms of currently available estrogen receptor-active compounds. Although the mechanics of ligand binding in estrogen receptors is generally well understood, there is room for surprises. In this paper computational evidence corroborating the experimentally observed type I agonistic binding mode for estradiol (E2) and diethylstilbesterol (DES) and the type II antagonistic binding mode for 4-hydroxytamoxifen and raloxifen is presented. Included in this type I agonistic mode are the DES derivatives, transstilbene and 1,2-diaryldiaminoethane. In addition, a novel 'type II agonistic' binding mode for 2,3-diarylimidazolines, 4,5-diarylimidazoles, 2,3-diarylpiperazines is introduced. This mode is stabilized by alternative hydrogen bond anchor points in the ligand binding domain as potential leads for future drug design.

1. Introduction

Estrogens play a decisive role in a network of processes including tissue growth and development, and are implicated in coronary heart disease, osteoporosis, and breast cancer.[1] Most of the effects are mediated by two intranuclear proteins, the estrogen receptors alpha (ERα) and beta (ERβ).[2] The receptors bind in vivo steroidal (e.g., estradiol (E2)), nonsteroidal estrogens (e.g., diethylstilbesterol (DES)), phytoestrogens (example: genistein (GEN)) but also compounds designed as antagonists and partial agonists (e.g., raloxifen (RAL) or 4-hydroxytamoxifen (4-OHT)) (Fig. 1). RAL and 4-OHT, are categorized as selective estrogen receptor modulators (SERMs). SERMs have very selective, antagonistic or agonistic tissue-dependent effects and may serve as therapeutic agents for breast cancer and osteoporosis.[3–5]

Estrogens can alter the folding of the ERα complex into two discrete shapes. The essentially planar estrogens, DES and derivatives like 1,2-diarylaminoethane (**2**), are defined as type I (class-1) estrogens, whereas angular estrogens based on triphenylethylenes or novel 2,3-diarylpiperazines (**4**) and 4,5-diarylimidazolines (**5**) (Fig. 2) are categorized as type II (class-2) estrogens.[1,6–9] Based on our findings, we additionally subdivide the type II compounds into agonistic and antagonistic classes, with the former containing the angular agonists and the latter describing molecules like 4-hydroxytamoxifen and raloxifen. Generally, binding of type I estrogens encourages the formation of the correct ER topology for cofactor binding at the Activity Factor 2 (AF2) site, while type II antagonists produce an activated AF2b site; both topologies promote estrogenic and partial estrogenic activity, respectively.[10,11] The exact topology formed upon type II agonist binding has not yet been established, though we would expect a conformation similar to type I.

Keywords: Estrogen receptor ligands; Molecular docking; Agonistic and antagonistic binding modes; Drug design; Anchor points; Binding pocket.
* Corresponding author. Tel.: +49 030 838 53272; fax: +49 030 838 53854; e-mail: knapp@chemie.fu-berlin.de

0968-0896/$ - see front matter © 2004 Elsevier Ltd. All rights reserved.
doi:10.1016/j.bmc.2004.09.022

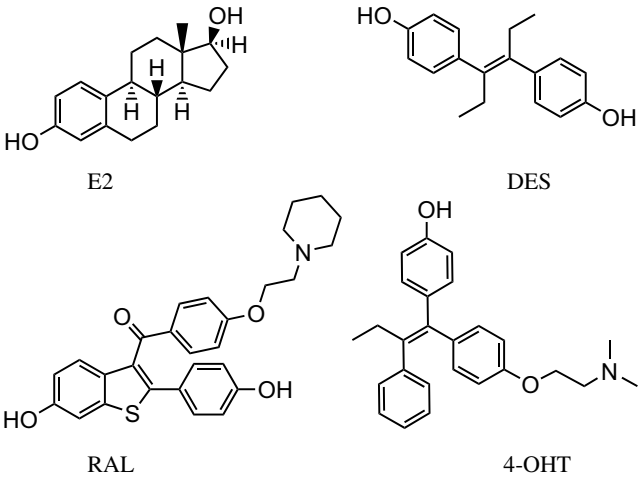

Figure 1. The molecular structure of estradiol (E2), diethylstilbesterol (DES), 4-hydroxytamoxifen (4-OHT), and raloxifen (RAL).

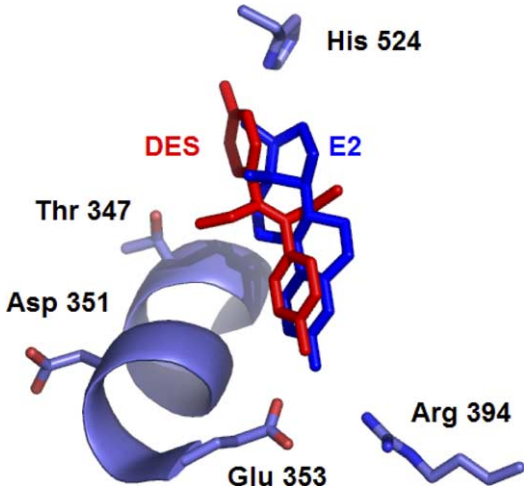

Figure 3. The type I binding mode exemplified by E2 and DES, whereby hydrogen bonds are formed with His524 and the Glu353/Arg394 pair.

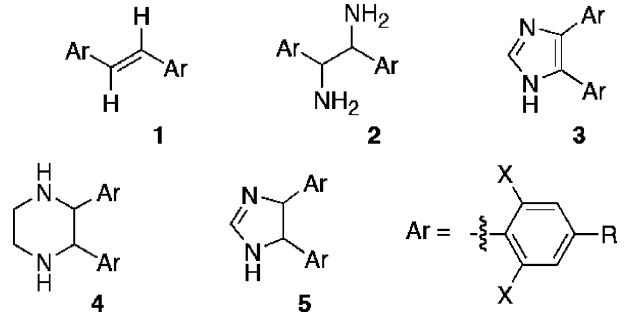

Figure 2. Molecular structures of the alkene (**1**), diamine (**2**), imidazole (**3**), imidazoline (**4**), and piperazine (**5**) test compounds. Ar signifies a substituted benzene ring, for which X can be either chlorine or fluorine, and R is either a hydroxyl or methoxy group.

The binding mode of type I estrogens can be deduced from the crystal structures of E2 and DES (Fig. 1) cocrystallized in the ligand binding domain (LBD) of the estrogen receptor.[12–14] The agonist type I binding mode demonstrated for DES and E2 is characterized by a hydrogen bond between the ligand's phenol group and the γ-carboxylate of Glu353, the Arg394 guanidinium entity as well as an additional hydrogen bond to the imidazole group of His524 (Fig. 3). This type I binding mode normally shifts helix H12 into a position antiparallel to helix H11 (Met517–Met528), thereby sealing the ligand in a hydrophobic core and exposing the LXXLL cofactor binding motif on the receptor surface.[15] Such estrogenic ligands promote conformational changes of the receptor that are conducive to dimerization and ultimately, interactions with target DNA sequences.[9] Alternatively, partial antagonists that dock in the LBD exhibit interactions with Asp351 on helix H3 and thereby prohibit the change into the transcriptionally active conformation of helix H12 (Fig. 4). The antagonistic binding mode is normally inaccessible in the protein structures of DES and E2, as the position of H12 occludes ligand access to Asp351.

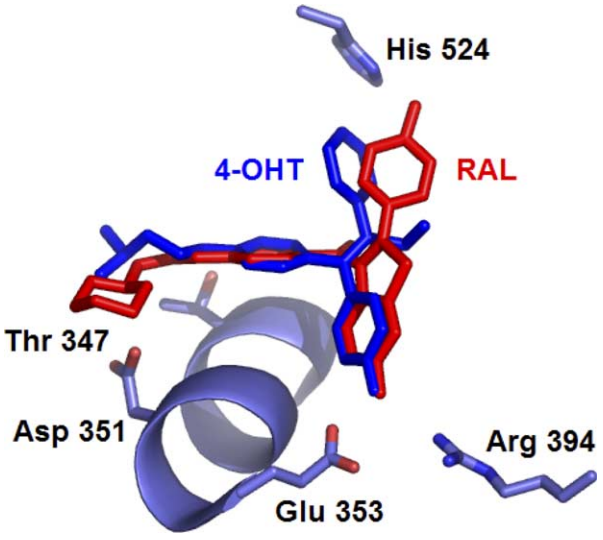

Figure 4. The type II antagonistic binding mode shared by 4-OHT and RAL, which is characterized by hydrogen bonding with Asp351 and the Glu353/Arg394 pair.

In addition to the above discussed binding modes a novel type II agonistic binding mode (Fig. 5) was postulated based on the relative binding activity (RBA) and luciferase activation data (Table 1) obtained for 2,3-diarylpiperazines, 4,5-diarylimidazolines, and 4,5-diarylimidazoles.[6] Gust and co-workers suggest that although these nonsteroidal compounds activate luciferase expression, RBA results indicate that displacement of the cognate E2 compound is negligible and therefore the analogs do not directly compete with E2 at its cognate binding site. Since these compounds lack the fused ring backbone characteristic of prototypical agonists yet still exhibit gene expression, another binding mode in the LBD is postulated. Computational studies outlined in this paper suggest binding is instead mediated through hydrogen bonding to Thr347 as opposed to His524.

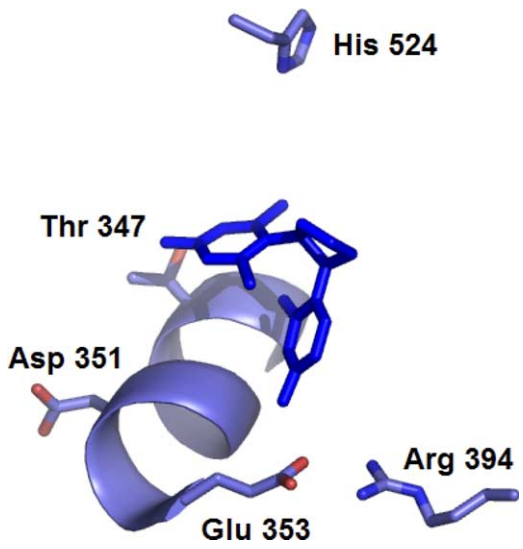

Figure 5. The type II agonistic binding mode postulated for the angular, type II ligands ((**3**), (**4**), and (**5**)) portrayed in Figure 2. This mode is stabilized by hydrogen bonding with Thr347 and the Glu353/Arg394 pair. Note that Asp351 is rotated away from the binding site in the agonist conformation of the ER.

Similar to a recent two step modeling study,[16] the coarse-grain docking algorithm, DOCK4.0,[17] was complemented with an energy optimization strategy using the CHARMM22 force field[18] and the Generalized Born (GB) solvation model to gauge the binding activity of a series of models of hormonally active compounds synthesized listed in Figure 2. The GB method represents the solvent as continuum dielectric. Thus, it effectively averages over different solvent conformations and can therefore be considered as an approximate free energy. In the past, docking studies have been performed for the estrogen receptor, utilizing both traditional,[19–21] explicit force field docking approaches as well as QSAR-reliant strategies.[22–24] Although QSAR studies performed in general remarkably well for numerous estrogenic compounds, we believe the QSAR models would not be well optimized for these compounds because we suspect an unconventional binding mode for the angular SERMS.

Proceeding rather with an explicit, all-atom force field docking strategy, we first demonstrate in this study that the ethylene and diamine structures, given their similarity to the DES structure, exhibit an energetic preference for the type I binding mode. In contrast, the angular SERMs, which are structurally unable to utilize the type I binding mode, alternatively are stabilized by the type II agonistic binding mode identified in this strategy. Additionally, it is shown that hydroxylated compounds report a much greater affinity than their methylated counterparts, which corroborates luciferase activation data (Table 1) recorded by Gust and co-workers.

2. Results

2.1. General aspects

To identify possible binding modes for ligands in the subsequent analysis, a docking survey was initially pursued. The conformational search employed by DOCK4.0[17] provides a fast and efficient means to explore the LBD of a fixed protein structure and its available ligand binding modes. Our strategy utilizes the receptor cocrystallized with the agonist DES (3erd[12]) and is therefore optimized for the planar, agonistic compounds considered in this study. However, the exact conformations of local residues within the binding site are likely to differ for the angular agonists, therefore binding data are likely to be falsely biased toward the planar compounds.

In this study, though the cognate compounds were predicted successfully by DOCK4.0, the predicted binding modes of the SERM compounds largely had unfavorable interaction energies, which could be due to the static model of the receptor. Therefore, our docking protocol was supplemented with a perturbation strategy that employs harmonic constraints to optimize binding for each of the represented binding modes. With this approach, the ligand was fixed in its active mode while the residues within the binding cavity relax to stabilize the compound. In this way, the structural bias of the estrogen receptor for DES can be overcome.

2.2. Validation of the docking procedure using known crystal structures

To determine the viability of the coarse-grained conformational search capability of DOCK4.0[17] for ER, the agonists DES and E2, as well as the antagonists RAL and 4-OHT, were blindly docked into the receptor LBD. Given that DOCK4.0 is conventionally limited to fixed protein docking approaches, the compounds were docked into their respective receptor conformations from the PDB, as the residues comprising the LBD are optimally positioned for binding these ligands. Such approaches have recently been employed to successfully predict the conformation and relative binding affinity of Phe versus the entire amino acids pool in phenylalanyl tRNA-synthetase[25] and the docking of active substrates into G protein receptors.[26,27]

Table 1. Relative binding affinity (as measured by E2 displacement) and luciferase activation values with respect to E2

Luciferase expression for representative compounds	Relative binding affinity [%]	Relative activation [%]	
		OH derivatives	OCH_3 derivatives
2,6Cl_2-4OH-2Cl-4OH imidazole[6]	0.00	27	6
2,6Cl_2-4OH-2Cl-4OH imidazoline[7]	0.08	112	6
2,6Cl_2-4OH-2Cl-4OH piperazine[8]	0.02	73	5

Table 2. Summary validation results for the agonists DES and ER, as well as the antagonists RAL and 4-OHT

Root mean square deviations for validation trials	RMSD	
	DOCK	Perturbed
Agonists		
Diethylstilbesterol (DES)	1.67	1.65
Estradiol (E2)	0.89	0.47
Antagonists		
Raloxifen (RAL)	0.62	0.60
4-Hydroxytamoxifen (4-OHT)	1.38	0.66

Using this blind docking procedure for the agonists, we found for DES a root mean square deviation (RMSD) with respect to the crystal structure of 1.67 Å in comparison to 0.89 Å for E2 (Table 2). The agonistic structures available in the PDB all support the type I binding mode, which relies on anchoring hydrogen bonds to His524 and the Glu353/Arg394 pair for stability. Thus, the predicted E2 conformation aligned with the cocrystallized structure, while the predicted DES structure deviated only in the positioning of the ethyl side chains of the bridge. The relatively large open space surrounding this midsection of the molecule gives rise to relatively weak interaction potentials, therefore the discrepancy was not unexpected.

Of the antagonists, the predicted 4-OHT structure was found with a 1.38 Å RMSD compared with the crystal structure, while RAL was found with an RMSD of 0.62 Å (Table 2). These structures resembled the described antagonistic binding mode, which again is based on contacts with Asp351 and the Glu353/Arg394 pair. Given these findings for the cognate compounds, we feel confident that the predicted binding modes from DOCK4.0 are sufficiently accurate for subsequent modeling.

2.3. Validation of perturbation strategy for known crystal structures

The top structures obtained from DOCK4.0[17] for the agonists E2 and DES and antagonists RAL and 4-OHT were perturbed via harmonic constraints into each described binding mode. Using the ER crystal structure (PDB code 3erd[12]) structure, only E2 and DES (Tables 2 and 3) converged to an optimized structure, yielding

Table 3. Summary of protein–ligand conformations and energies (in kcal/mol) in absence of solvent

Ligand/binding mode	Summary of perturbation conformation data									
	Normal		PIA		PIIX		PIIA		PIIA-347	
Diethylstilbesterol (DES)			**I**	**−52.2**						
Estradiol (E2)			**I**	**−45.1**						
1-(2,6Cl_2-4OH-Ph)-2-(2F-4OH-Ph) (*E*)	I	−43.9	I	−51.3	I	−43.9	I	−47.0	**I**	**−52.0**
1-(2,6Cl_2-4OH-Ph)-2-(2Cl-4OH-Ph) (*E*)	I	−39.3	I	−39.7	D	−46.4	I	−49.9	**I**	**−52.8**
1-(2,6Cl_2-4OMe-Ph)-2-(2Cl-4OMe-Ph) (*E*)	D	−44.5	D	−47.1	D	−48.7	**I**	**−38.6**	D	−37.3
1-(2,6Cl_2-4OMe-Ph)-2-(2Cl-4OMe-Ph) (*Z*)	D	−31.4	D	−47.5	D	−52.6	**I**	**−55.6**	I	−42.3
1-(2,6Cl_2-4OH-Ph)-2-(2Cl-4OH-Ph) (*e*)	I	−50.3	I	−52.6	D	−42.9	D	−33.3	**I**	**−52.0**
1-(2,6Cl_2-4OH-Ph)-2-(2Cl-4OH-Ph) (*t*)	I	−47.6	I	−49.1	D	−39.8	I	−48.2	**I**	**−49.1**
1-(2,6Cl_2-4OMe-Ph)-2-(2Cl-4OMe-Ph) (*e*)	D	−51.2	I	−37.8	D	−47.5	**I**	**−40.0**	D	−39.8
1-(2,6Cl_2-4OH-Ph)-2-(2Cl-4OH-Ph) (*t*,*SS*)	**I**	**−54.8**	I	−48.9	D	−36	D	−44.5	II	−50.1
1-(2,6Cl_2-4OH-Ph)-2-(2F-4OH-Ph) (*e*,*SR*)	I	−55.3	**I**	**−57.1**	D	−45.1	D	−50.0	I	−56.0
1-(2,6Cl_2-4OMe-Ph)-2-(2Cl-4OMe-Ph) (*e*,*SR*)	**I**	**−56**	I	−55.6	D	−57.5	II	−57.5	II	−47.8
1-(2,6Cl_2-4OH-Ph)-2-(2Cl-4OH-Ph) (*e*,*SR*)	I	−54.9	**I**	**−56.4**	D	−44.1	I	−52.4	II	−42.7
4-(2Cl-4OH-Ph)-5-(2,6Cl_2-4OH-Ph)	D	−47.3	D	−49.4	D	−40.3	D	−44.8	**II**	**−46.9**
4-(2Cl-4OMe-Ph)-5-(2,6Cl_2-4OMe-Ph)	D	−47.0	D	−45.0	D	−38.1	D	−41.1	**II**	**−43.2**
4-(2F-4OH-Ph)-5-(2,6Cl_2-4OH-Ph)	D	−32.7	I	−37.1	D	−22.2	D	−32.0	**II**	**−42.5**
2-(2,6Cl_2-4OH-Ph)-3-(2Cl-4OH-Ph) (*e*)	**II**	**−41.5**	I	−43.9	D	−42.6	D	−40.2	II	−34.3
2-(2F-4OH-Ph)-3-(2,6Cl_2-4OH-Ph) (*e*)	D	−48.1	D	−39.2	D	−47.6	**II**	**−51.4**	D	−51.5
2-(2F-4OH-Ph)-3-(2,6Cl_2-4OH-Ph) (*e*,*SR*)	D	−42.8	D	−33.7	D	−40.5	D	−42.9	**II**	**−42.9**
2-(2Cl-4OMe-Ph)-3-(2,6Cl_2-4OMe-Ph) (*t*)	D	−47.9	D	−47.7	D	−45.8	D	−51.8	**II**	**−42.4**
2-(2,6Cl_2-4OH-Ph)-3-(2Cl-4OH-Ph) (*e*,*S*)	D	−40.3	D	−45.9	D	−43.7	D	−47.3	**II**	**−48.6**
2-(2Cl-4OMe-Ph)-3-(2,6Cl_2-4OMe-Ph) (*e*,*S*)	D	−41.1	D	−42.7	D	−39.4	D	−42.7	D	−39.1
2-(2,6Cl_2-4OH-Ph)-3-(2Cl-4OH-Ph) (*t*,*SS*)	D	−39.4	D	−33.7	D	−43.5	D	−40.5	**II**	**−44.2**
2,3-Bis(2,6Cl_2-4OH-Ph) (*m*)	D	−42.9	D	−43.0	I	−41.2	D	−39.4	**II**	**−43.1**
2,3-Bis(2,6Cl_2-4OMe-Ph) (*m*)	D	−50.1	D	−50	D	−46.3	D	−46.2	**II**	**−49.1**
2-(2F-4OH-Ph)-3-(2,6Cl_2-4OH-Ph) (*e*,*SR*)	D	−45.5	D	−43.8	D	−39.8	**II**	**−45.0**	D	−44.0
2-(2Cl-4OH-Ph)-3-(2,6Cl_2-4OH-Ph) (*e*,*SR*)	D	−46.9	D	−45.8	D	−45.0	D	−46.8	**II**	**−44.0**
2,3-Bis(2,6Cl_2-4OMe-Ph) (*m*)	D	−47.8	D	−46.8	D	−48.4	**II**	**−51.1**	D	−47.8

Aside from the unperturbed (normal) conformation (second column) the perturbed conformations were considered as starting structures for structural relaxation (next five columns). PIA corresponds to a ligand perturbed to the type I agonistic binding mode, PIIA and PIIX represent perturbations to the type II agonistic (3erd[12]) and antagonistic (1ere) receptors, respectively. PIIA-347 signifies the type II agonistic binding mode using the rotated Thr347 residue. The ligand conformations and energies obtained after the constraints were released and the ligand structure minimized are listed as agonistic type I (I) and type II (II), as antagonistic (X), or as distorted (D) binding mode. The text in bold represents calculated results that reported low energies.

type I binding modes. The E2 conformation relaxed with the CHARMM22[18] energy function had an RMSD from the crystal structure of 0.47 Å, while for DES 1.65 Å was obtained, which are both slight improvements over the results obtained with DOCK4.0.[17] For the antagonistic structures, on the other hand, suitable binding conformations were achieved only when docked into the ER structure with PDB code 1err,[14] for which helix H12 was translocated into its antagonistic orientation thereby exposing Asp351. These compounds were subsequently relaxed with the CHARMM22[18] energy function, yielding RMSD values of 0.66 and 0.60 Å for 4-OHT and RAL (Table 2), respectively. These results suggest that the H12 displacement is critical for hydrogen bonding to Asp351 and ultimately for antagonist recognition. Lastly, all successfully modeled compounds were docked and perturbed with negligible disturbance of H12 during the course of energy minimization, thereby suggesting the stability of the respective agonist and antagonist modes of the ER.

2.4. Results for DES derivatives

The following compounds were modeled according to the procedure outlined for the crystal structures, which yielded good agreement with experimental data. Supplementing the docked structures with the described perturbation strategy enables the isolation of the most plausible binding modes for a given SERM. In Table 3, the energies of the ligands perturbed into the possible binding modes are summarized, with the lowest energy mode designated as the native mode for binding affinity comparisons.

2.5. Stilbenes

These structures are highly similar to DES, differing only in the substitution of ethyl groups for hydrogens on the bridging group and the halogens in the *ortho* positions of the substituent phenyl groups (**1**) (Fig. 2). The bridging group double bond fixes the phenyl rings in an extended orientation (Fig. 6), whereby the phenols interact with His524 and the Glu353/Arg394 pair. This conformation limits type I binding as the only feasible option for stabile anchoring (Table 4). Further stabilization of the ligand binding was mediated by contact with the hydrophobic residues Ala350, Leu387, Leu391, and Phe404, which form a tight pincer arrangement near Arg394 and Glu353, while the residues Met421, Gly521, and Leu525 form a loose pincer near His524 (Table 5). Although the O-methylated compounds preferred the type I conformation and were stabilized by the same pincer arrangement for the hydroxylated compounds, the lack of hydrogen bonding capabilities greatly reduced their overall binding affinities. Thus, the O-methylated structures reported a binding affinity roughly 30 kcal/mol less than that for the hydroxylated cases.

2.6. Diamines

The 1,2-diaminoethane substructure (**2**) (Fig. 2) introduces a larger steric term in the LBD, as well as a polar contribution from the amines. Similar to the stilbenes

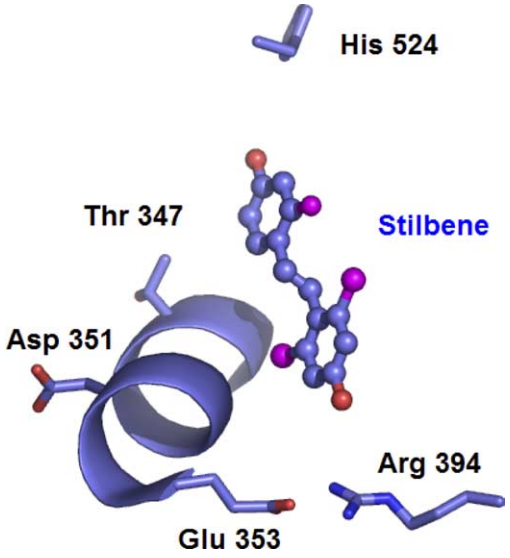

Figure 6. An example stilbene compound stabilized in the type I binding mode. This mode is traditionally preferred for the cognate E2 and DES, as well as the stilbene and diamine structures examined in this study.

(Fig. 6), these compounds were stabilized through the type I binding mode, although with a lesser affinity (Table 4). The high affinity was again largely driven by the vise-like arrangements of the hydrophobic residues near the anchoring points. However, the binding of diaminoethanes is weaker than that of stilbenes, since there is an additional cost for desolvating the polar amines that is not sufficiently counterbalanced by interactions with the hydrophobic residues in the bridging area. As was similarly observed for the stilbenes, the O-methylated diamines assumed type I binding modes as well, but again demonstrate lesser affinity (approx. 10–20 kcal/mol) than their hydroxylated counterparts.

2.7. Imidazoles

The imidazoles energetically preferred the type II agonistic binding mode (Table 6, Fig. 7), relying on hydrogen bonding with Thr347 instead of His524 and the Glu353/Arg394 pair. In this binding mode, the phenyl ring proximal to Thr347 is instead stabilized by another comparable vise-like arrangement of residues Met343, Leu346, Met421, and Leu525 while there is no change in the stabilizing interactions with the hydrophobic residues near Glu353/Arg394 (Table 5). This alternative arrangement is due to the ethene substructure of the imidazole ring, which forces the rings of the ligand into a *cis* arrangement that prevents interaction with His524. For this subclass of structures, the binding affinities of the hydroxylated as compared to the methylated compounds was especially pronounced. With a difference of approximately 35 kcal/mol, this would explain the substantial difference in luciferase expression (27% vs 6%) with respect to E2 (Table 1).

2.8. Imidazolines

Like the imidazoles, the imidazoline structures preferred the type II agonistic binding mode (Table 6) as shown in

Table 4. Predicted binding mode and binding affinities for the structures exhibiting the type I binding mode

Binding conformations and affinities of type I structures	Binding mode	Binding energy
Cognate		
Diethylstilbesterol (DES)	Type I	−65.15
Estradiol (E2)	Type I	−56.14
Alkenes		
1-(2,6Cl_2-4OH-Ph)-2-(2F-4OH-Ph) (*E*)	Type I	−77.31
1-(2,6Cl_2-4OH-Ph)-2-(2Cl-4OH-Ph) (*E*)	Type I	−76.00
1-(2,6Cl_2-4OMe-Ph)-2-(2Cl-4OMe-Ph) (*Z*)	**Type I**	**−45.73**
1-(2,6Cl_2-4OMe-Ph)-2-(2Cl-4OMe-Ph) (*E*)	**Type I**	**−44.18**
Diamines		
1-(2,6Cl_2-4OH-Ph)-2-(2Cl-4OH-Ph) (*e*,*SR*)	Type I	−64.12
1-(2,6Cl_2-4OH-Ph)-2-(2F-4OH-Ph) (*e*,*SR*)	Type I	−63.79
1-(2,6Cl_2-4OH-Ph)-2-(2Cl-4OH-Ph) (*t*,*SS*)	Type I	−63.13
1-(2,6Cl_2-4OH-Ph)-2-(2Cl-4OH-Ph) (*e*)	Type I	−60.64
1-(2,6Cl_2-4OH-Ph)-2-(2Cl-4OH-Ph) (*t*)	Type I	−58.69
1-(2,6Cl_2-4OMe-Ph)-2-(2Cl-4OMe-Ph) (*e*,*SR*)	**Type I**	**−51.24**
1-(2,6Cl_2-4OMe-Ph)-2-(2Cl-4OMe-Ph) (*e*)	**Type I**	**−41.32**

The binding affinities listed include solvation. The text in bold correspond to the methylated compounds.

Table 5. Summary of key residue interactions for the canonical binding modes

Mode	Stabilizing residues according to binding mode	
	Hydrogen bonding residues	van der Waals residues
Type I	H524, E353, R394	M421, G521, L525, A350, L387, L391, F404
Type II	T347, E353, R394	M343, L346, M421, L525, A350, L387, L391, F404

Table 6. Predicted binding mode and binding affinities for the structures exhibiting the type II binding mode

Binding conformations and affinities of type II structures	Binding mode	Binding energy
Imidazoles		
4-(2F-4OH-Ph)-5-(2,6Cl_2-4OH-Ph)	Type II	−43.34
4-(2Cl-4OH-Ph)-5-(2,6Cl_2-4OH-Ph)	Type II	−43.32
4-(2Cl-4OMe-Ph)-5-(2,6Cl_2-4OMe-Ph)	**Type II**	**−18.69**
Imidazolines		
2-(2F-4OH-Ph)-3-(2,6Cl_2-4OH-Ph) (*e*)	Type II	−44.30
2-(2,6Cl_2-4OH-Ph)-3-(2Cl-4OH-Ph) (*t*,*SS*)	Type II	−43.53
2-(2,6Cl_2-4OH-Ph)-3-(2Cl-4OH-Ph) (*e*)	Type II	−40.98
2-(2,6Cl_2-4OH-Ph)-3-(2Cl-4OH-Ph) (*e*,S)	Type II	−31.91
2-(2Cl-4OMe-Ph)-3-(2,6Cl_2-4OMe-Ph) (*t*)	**Type II**	**−27.94**
2-(2Cl-4OMe-Ph)-3-(2,6Cl_2-4OMe-Ph) (*e*,*S*)	**Type II**	**−19.14**
2-(2F-4OH-Ph)-3-(2,6Cl2-4OH-Ph) (*e*,*SR*)	Type II	−16.68
Piperazines		
2,3-Bis(2,6Cl_2-4OH-Ph) (*m*)	Type II	−47.57
2-(2Cl-4OH-Ph)-3-(2,6Cl_2-4OH-Ph) (*e*,*SR*)	Type II	−47.20
2-(2F-4OH-Ph)-3-(2,6Cl_2-4OH-Ph)	Type II	−46.09
2,3-Bis(2,6Cl_2-4OMe-Ph) (*m*)	**Type II**	**−36.87**
2-(2Cl-4OMe-Ph)-3-(2,6Cl_2-4OMe-Ph) (*e*,*SR*)	**Type II**	**−25.12**

The binding affinities listed include solvation. The text in bold correspond to the methylated compounds.

Figure 7, with binding affinities comparable to the imidazoles. The bridging groups differ only slightly, in that the imidazole double bond is substituted for a single bond in the imidazoline structures, which thereby induces a very slight conformational rearrangement of the bridging group. This alteration does not seem to impact the predicting binding affinity to any large degree.

Whereas all other imidazolines preferred pointing the heterocyclic bridging group toward Met388, 2F-4OH-2,6Cl_2-4OH (*e*,*SR*) was an exception to this trend as it positioned the hetero-atoms of the bridging group toward Met421. This positioning resulted in nonoptimal placement of the phenols, therefore greatly compromised the anchoring hydrogen bonds and moreover, reduced the overall binding affinity. This observation suggests that stereochemistry may play a key role in activation of the ER.

Additionally, the trend that hydroxylated structures are favored over their O-methylated counterparts surfaces among these data as well, although with a separation

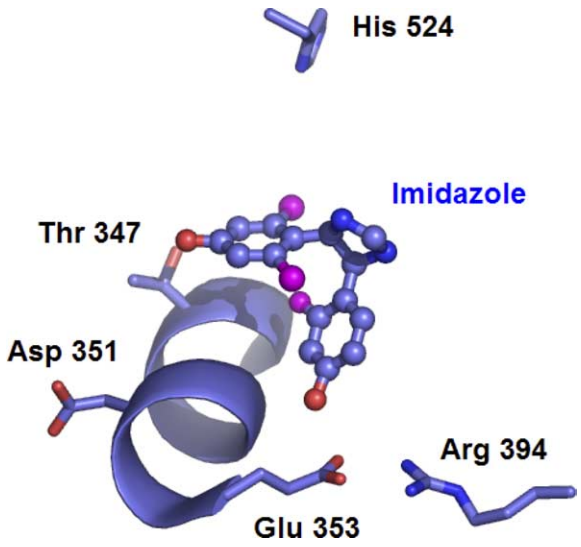

Figure 7. A representative imidazole compound, which is stabilized by the type II binding mode. This mode of binding was also observed for other angular compounds, including the imidazolines and piperazines.

of only 5–12 kcal/mol. This agrees with the activity data (112% vs 6%) (Table 1), though it is surprising that such a large difference in activity was not also reflected in the computed binding affinities.

2.9. Piperazines

As with the imidazolines, these compounds preferred the type II agonistic binding mode (Table 6), similar to the mode portrayed in Figure 7. The piperazine structures have a slightly larger heterocyclic ring than the preceding imidazole derivatives, which may account for the increased binding affinity compared to the imidazole-based ligands. All minimized structures pointed with the heterocyclic ring toward Met388, which further suggests the possible role of stereochemistry in stabilizing the ligand. Again the O-methylated compounds were reduced in binding energy by 10–20 kcal/mol, in accordance with the observed luciferase activity difference of 73% versus 5% (Table 1).

3. Discussion

3.1. Binding modes

The type I binding mode is ideal for DES and E2, whereby the phenyl rings are constrained in an extended conformation by the bridging group (Fig. 3). The extended conformation of DES and E2 is conducive to forming contacts with the type I binding mode anchoring residues, which are arranged linearly within the LBD. The stilbenes and 1,2-diaminoethanes at the focus of this study bear remarkable structural similarity to these cocrystallized compounds with only minimal changes in the bridging group. These respective bridging groups place the anchoring phenyl groups in similar positions as those of DES and E2. Thus, little structural reorganization of the LBD was required to support the binding of these molecules.

The antagonistic binding mode is normally inaccessible in the protein structures of DES and E2. Helix H12, which is ideally situated for cofactor binding in these cocrystallized structures, typically occludes ligand access to Asp351, a necessary component for type II antagonistic binding. As previously mentioned, Leu540 is the most apparent impediment to the formation of a hydrogen bond with Asp351. Suitable hydrogen bond distances cannot be attained without disturbing the backbone of Leu540 and likewise of helix H12. Although it is possible that these components must be shifted to allow for accommodation of a ligand in the antagonistic binding mode, it is not obvious from our approach how the resulting structure would affect the cofactor recognition surface.

The type II agonistic binding mode appears to offer the most viable position for the imidazole, imidazoline, and piperazine structures, whose bridging groups force the phenyl rings into bent conformations. This bending does not promote interaction with His524. Instead Thr347 provides reasonable hydrogen bonding to the bent ligand hydroxyl groups. Binding in this fashion induces negligible shifting in the position of helix H12, which suggests its agonistic functionality. Lastly, there appears to be a homologous threonine in the ERβ substructure at position 399, which introduces the possibility of type II agonistic binding for the structure as well.

3.2. General observations

No trends in the binding data were observed that illustrated a preference for di-chlorination on one phenol versus the other. The binding cavity directly adjacent to the bridging group is comparatively open with regards to the pincer arrangements found at either anchoring residue. Therefore, considerable flexibility in the size of the phenyl substitutions was permitted. Additionally, there was also no clear preference for fluorination versus chlorination according to our computations. However, given that the force field parameters for the halogens may not be well optimized for such compounds, computations may not readily differentiate patterns of halogenation.

As indicated by the binding data for the hydroxylated versus the methylated compounds, a successfully bound ligand requires the substituent phenol groups to be positioned close to the anchoring residues. To this end, the nature and stereochemistry of the bridging group governs the placement of the phenyl groups and moreover, define the binding mode for a given compound. The predicted structures from this study largely preferred the hetero-atoms of the bridging group to either be collinear with the phenyl ring atoms or pointing toward Met388. Compounds whose stereochemistry

forced the ring toward Met421 were noticeably less stable. Regardless of stereochemistry, compounds overwhelmingly prefer to align with the defined type II anchoring points.

Unfortunately, though the computed binding data clearly identify binding modes and distinguish between hydroxylated and methylated compounds, minute differences in bridging group and stereochemistry were not well addressed. To accomplish this, the force field will likely need to be supplemented with additional valence and nonbonded interaction terms to accurately account for strain and steric problems. Additionally, the issue of side chain conformations would be better answered by using an accurate side chain placement program to guarantee the optimal binding site for a given ligand.

3.3. Pharmacophore requirements

For the future development of potentially active SERMs, several factors clarified by this study should be considered:

(1) The vise-like arrangement of the hydrophobic quartet Ala350, Leu387, Leu391, and Phe404, neighboring the Glu353/Arg394 pair, as well as those residues proximal to the type I and type II agonistic anchoring points, that is, the Met421/Gly521/Ala350 set for His524 and the Met343/Leu346/Met421/Leu525 quartet for Thr347, are crucial for stabilizing the hydrophobic portions of the ligand anchors. Furthermore, the cavities formed by these vises appear to be selective for planar, ring-like structures, which make phenols ideal for anchoring ligands.

(2) The hydrophobic residues constituting the midsection of the LBD, namely Leu346, Ala350, and Leu384 for type I binding and residues Leu384, Met388, and Leu428 for type II agonistic binding, offer large flexibility in the nature of the bridging functional group. Modifying the relative size of the bridging group and its degree of hydrophobicity varies the strength of interaction with these LBD residues.

(3) As for the bridging group of the ligand, agonistic activity could be favored for structures that orient the anchoring phenyl rings for optimal interactions conducive to type I or type II agonistic binding. Large substitutions on the bridging group, which may pierce the enclosed binding domain, such as for 4-OHT and RAL, prevent full closure of helix H12 against the hydrophobic LBD, or binding in the type II agonistic mode could induce possible antagonistic or partial agonistic behavior.

(4) The apparent role of the negatively charged Asp351 residue in cofactor recognition could prove especially useful in modulating the agonistic versus antagonistic nature of potential SERMs. Moieties that preserve the Asp351 position would likely promote estrogenic action, whereas functional groups that effectively interact with and shield this residue[28] should exhibit inhibitory effects for ER. It should be additionally noted that none of the considered compounds exhibited favorable binding interactions with this Asp351 in the agonist conformation of the ER.

4. Conclusions

This study demonstrates that the LBD of ER supports a number of binding modes for agonists and antagonists, and readily incorporates a significant range of ligand sizes and conformations. These findings fully corroborate the observation that the ER binding pocket is very general in its selectivity of binding ligands.[13] The molecular docking strategy outlined in this paper has provided computational evidence for verifying the type I binding mode for planar agonists and introduced the possibility of an agonistic type II binding mode for angular ligands. In addition, analysis of the residues that stabilize the ligands in the binding modes could open new directions in the design of SERMs. Furthermore, given the similarity of the estrogen receptor to other receptors of the nuclear receptor family, this computational approach could be equally applicable for determining the binding modes and agents for other related receptors.

5. Methods

5.1. Docking strategies

The coarse-grained conformations obtained with DOCK4.0[17] using its explicit energy function[29] served primarily to provide a reasonable guess of the ligand conformations in the LBD, both for the protein structure catered in the fixed conformation of the crystal structure cocrystallized with the agonists DES and E2, available in the Protein Data Bank (PDB) (code 3erd[12] and 1ere[14]), as well as in the protein conformation optimized with CHARMM[18,30] for the antagonists RAL and 4-hydroxytamoxifen (4-OHT). Since we are testing for agonistic activity of the drug candidates, the conformational search is based on the agonistic protein structure cocrystallized with DES, which has a backbone conformation optimized for this binding mode and moreover an ideal position of helix H12 for transcriptional activity.

The top 10–15 scored conformations from a DOCK4.0[17] trial run were further optimized with a flexible protein model employing the energy minimization algorithm in CHARMM.[18] The minimization routine consisted of 500 Steepest Descent steps, followed by 2000 Newton–Raphson steps, all without including solvation forces, which would have considerably slowed the computations. This relaxation technique allows for the protein to adjust slightly to the bound ligand with minimal disturbance of the binding mode predicted by DOCK4.0.

5.2. Cross-perturbation

Cross-perturbation, that is, guiding a given structure into the binding conformations of other related structures, is a useful and effective strategy to expand the conformational search with active ligand conformations. This method has been successfully used to rank the

binding of the 20 natural amino acids to the phenylalanyl-tRNA synthetase[25] with respect to observed k_{cat}/k_m AMP activation data.[31] For such correlations, the amino acids were required to assume positions conducive to ATP activation, which were generally not identified by docking. Since this study seeks to discriminate between agonistic and antagonistic activity of estrogen-related compounds, such perturbation strategies toward active binding modes are justified.

To this end, the binding geometry of the ligands were perturbed to each of the three binding modes considered in the present study (the agonistic type I and type II as well as the antagonistic binding modes) using suitable harmonic constraints available in CHARMM,[30] which promote the key anchoring atoms to assume normal hydrogen bond distances between 2.0 and 4.0 Å. These structures are then relaxed by the aforementioned energy minimization without constraints to avoid structural artifacts.

5.3. Preparation of structures

The structures of the DES derivatives considered in this study were optimized using the CHARMM22[18] all-atom force field. The atomic partial charges of the protein moiety were taken from CHARMM22,[18] for the drug molecules Gasteiger–Hückel[32] atomic partial charges were used. The ER cocrystallized structures used, 1ere and 1err[14] as well as 3erd and 3ert[12] were obtained from the PDB. Hydrogen atoms were added to the protein structure using the HBUILT procedure of CHARMM.[30] All Arg, Lys, Glu, and Asp residues were in their standard protonation state at neutral pH and His was assumed to be in the neutral charge state with Nδ protonated. To avoid uncertainties in the positions of hydrogen atoms explicit water molecules were removed based on our conclusions in previous studies.[33]

As the protein conformation used in this study was catered to binding the DES ligand, it was necessary to slightly rotate the side chains of Thr347 within the binding pocket such that access to the proposed anchoring residues could be facilitated. The Thr347 hydroxyl group is normally slightly buried according to the crystal structure of ER cocrystallized with DES. In this orientation, Thr347 forms a hydrogen bond with Gly344, though glycine appears to also be stabilized by hydrogen bonds with Asn348 and Tyr537. Alternatively, this hydroxyl group may energetically prefer to stabilize ligands incapable of binding to His524 than to remain buried in this region, therefore the hydroxyl group of Thr347 was rotated using harmonic constraints to face toward the binding pocket. This structure was then fully relaxed in the absence of constraints using energy minimization in CHARMM[30] with 700 steps of steepest descent and 5000 Newton–Raphson steps. The resulting protein structure with the rotated Thr347 was about 10 kcal/mol higher in energy than the original structure, but for a protein with an overall energy on the order of −4000 kcal/mol, this energy difference is not significant.

5.4. Protocol of docking procedure

The binding site of ER was scanned for possible binding modes, ignoring any bias from the binding geometry of the ligands in the available crystal structures. The employed docking protocol has been shown to efficiently scan an entire receptor for all possible binding sites without any structural bias.[25] This scanning procedure is based on docking simulations using DOCK4.0[17] combined with fine-grained CHARMM[30] molecular mechanic techniques. The corresponding docking protocol is comprised of the following steps:

(1) *Mapping the protein surface*: A probe of 1.4 Å radius was used to trace a 4 dots/Å^2 negative image of the protein molecular surface, according to Connolly's method.[34] The resulting data were used to generate clusters of overlapping spheres with the SPHGEN[35] program. The resulting representation of the protein surface served as basis for the docking method.

(2) *Definition of the docking region*: The pockets of empty space of the receptor surface represented by spheres near to the known binding site were selected as the search window for DOCK4.0.[17] Previous studies have already demonstrated[26] DOCK4.0's ability to locate a binding region on entire protein surfaces without structural bias.

(3) *Generation of docked conformations for the ligand–receptor complex*: The orientations of the ligand on the receptor surface were generated by DOCK4.0,[17] using flexible docking with torsion angle minimization of the ligand, a homogeneous dielectric with $\varepsilon = 2.5$ and a distance cutoff of 10 Å for the evaluation of nonbonded energy terms. In this way 3000 conformations were generated and ranked according to the DOCK4.0[17] energy function, which includes electrostatic and van der Waals terms, and only the highest ranking structure for each ligand was kept for further optimization, since the top 10–15 scored structures varied little in conformation. The remaining conformations had unfavorable energies dominated by unfavorable van der Waals interactions with the protein.

(4) *Optimization of the docking complexes*: The top-ranking structures obtained with DOCK4.0[17] were subjected to further optimization, using the more detailed all-atom force field from CHARMM22.[18] The first stage of optimization utilized a fully flexible ligand with fixed protein atoms with the implicit solvent model based on the GB continuum electrostatics. This was followed by an optimization with a flexible binding region, which was defined as the area within 10 Å of the bound ligand. Lastly, the resulting structures were fully relaxed without constraints. Each of the geometry optimization steps was performed by an energy minimization with 700 steps of steepest-descent and 5000 steps of Newton–Raphson.

(5) *Perturbation and relaxation of the docking complexes*: The docked conformations from step 4 were assigned harmonic constraints within the CHARMM[30] program.

These were used to pull the ligand hydroxyl groups within hydrogen bonding distance (2.0–4.0 Å of nonhydrogen atom distance) of the respective anchoring residues (of the type I, type II agonistic, or type II antagonistic binding mode) in a stepwise fashion, identical to the optimization procedure described in the above step of the docking protocol. The final structures were relaxed without constraints as in the preceding step 4 of the docking protocol.

(6) *Cross-perturbation*: Structures which did not yield useful conformations in step 3 of the docking protocol (in particular the methylated compounds) were perturbed into the coordinates of their hydroxylated counterparts. These were then optimized according to steps 4 and 5.

(7) *Selection of candidates*: The resulting conformations from step 6 were screened based on the binding energy computed in gas phase and whether or not hydrogen bonds (distance of the donor acceptor nonhydrogen atom pair smaller than 4.0 Å) were established to the characteristic anchoring residues of the various binding modes. The 'winners' for each compounds were subjected to single point energy calculations including the GB solvation model.

(8) *Ranking of ligand affinities*: The relative binding energies for the best ligand conformations were defined as the energy difference between the protein–ligand complex versus the energy of the same conformation of the lone ligand and protein in solution given by

$$\Delta\Delta G_{\text{calc}} = \Delta G_{\text{protein+ligand}} - [\Delta G_{\text{protein}} + \Delta G_{\text{ligand}}], \quad (1)$$

where $\Delta G_{\text{protein+ligand}}$, $\Delta G_{\text{protein}}$, and ΔG_{ligand}, are the computed energies for the protein–ligand complex, the protein, and the lone, solvated ligand, respectively. These energies include solvation effects using the GB continuum solvent approximation with a dielectric constant of 2.5 for the protein and 79.8 for the solvent. Nevertheless, because some entropic effects like different hydrogen bind pattern are neglected, they cannot be considered as complete free energies. Additionally, since the same protein and ligand conformations were used for computing both the complexed and isolated molecules, explicit contributions from bond, bond angle, and torsion angle energy terms were ignored. This helps to avoid artifacts in the internal energy that may arise solely from the minimization procedure but do not reflect actual relaxation of the isolated components. As such, the vertical binding affinity provides an upper limit of the actual binding energy, since structural relaxation effects upon separating the complex are neglected.

Acknowledgments

P.M.K.-H. greatly thanks the Fulbright Commission for supporting this work and cultural exchange. This work was supported by the Deutsche Forschungsgemeinschaft SFB 498, project A5, project Kn329/5-1, the graduate colleges GRK 80/2, GRK 268, and GRK 788/1, the Fonds der Chemischen Industrie and the BMBF.

References and notes

1. Jordan, V. C.; Gapstur, S.; Morrow, M. *J. Natl. Cancer Inst.* **2001**, *93*, 1449.
2. Gustafsson, J. A. *J. Endocrinol.* **1999**, *163*, 379.
3. Dutertre, M.; Smith, C. L. *J. Pharmacol. Exp. Ther.* **2000**, *295*, 431.
4. Rosati, R. L.; Jardine, P. D.; Cameron, K. O.; Thompson, D. D.; Ke, H. Z.; Toler, S. M.; Brown, T. A.; Pan, L. C.; Ebbinghaus, C. F.; Reinhold, A. R.; Elliott, N. C.; Newhouse, B. N.; Tjoa, C. M.; Sweetnam, P. M.; Cole, M. J.; Arriola, M. W.; Gauthier, J. W.; Crawford, D. T.; Nickerson, D. F.; Pirie, C. M.; Qi, H.; Simmons, H. A.; Tkalcevic, G. T. *J. Med. Chem.* **1998**, *41*, 2928.
5. Jordan, V. C. *J. Med. Chem.* **2003**, *46*, 1081.
6. Gust, R.; Keilitz, R.; Schmidt, K. *J. Med. Chem.* **2001**, *44*, 1963.
7. Gust, R.; Keilitz, R.; Schmidt, K.; von Rauch, M. *J. Med. Chem.* **2002**, *45*, 3356.
8. Gust, R.; Keilitz, R.; Schmidt, K. *J. Med. Chem.* **2002**, *45*, 2325.
9. Jordan, V. C.; Schafer, J. M.; Levenson, A. S.; Liu, H.; Pease, K. M.; Simons, L. A.; Zapf, J. W. *Cancer Res.* **2001**, *61*, 6619.
10. Nilsson, S.; Makela, S.; Treuter, E.; Tujague, M.; Thomsen, J.; Andersson, G.; Enmark, E.; Pettersson, K.; Warner, M.; Gustafsson, J. A. *Physiol. Rev.* **2001**, *81*, 1535.
11. Bentrem, D.; Fox, J. E.; Pearce, S. T.; Liu, H.; Pappas, S.; Kupfer, D.; Zapf, J. W.; Jordan, V. C. *Cancer Res.* **2003**, *63*, 7490.
12. Shiau, A. K.; Barstad, D.; Loria, P. M.; Cheng, L.; Kushner, P. J.; Agard, D. A.; Greene, G. L. *Cell* **1998**, *95*, 927.
13. Pike, A. C. W.; Brzozowski, A. M.; Hubbard, R. E.; Bonn, T.; Thorsell, A. G.; Engstrom, O.; Ljunggren, J.; Gustafsson, J. K.; Carlquist, M. *EMBO J.* **1999**, *18*, 4608.
14. Brzozowski, A. M.; Pike, A. C. W.; Dauter, Z.; Hubbard, R. E.; Bonn, T.; Engstrom, O.; Ohman, L.; Greene, G. L.; Gustafsson, J. A.; Carlquist, M. *Nature* **1997**, *389*, 753.
15. Pettersson, K.; Gustafsson, J. A. *Annu. Rev. Physiol.* **2001**, *63*, 165.
16. Hoffmann, D. K. B.; Washio, T.; Steinmetzer, T.; Rarey, M.; Lengauer, T. *J. Med. Chem.* **1999**, *42*, 4422.
17. Ewing, T. J. A.; Kuntz, I. D. *J. Comput. Chem.* **1997**, *18*, 1175.
18. MacKerell, A. D.; Bashford, D.; Bellott, M.; Dunbrack, R. L.; Evanseck, J. D.; Field, M. J.; Fischer, S.; Gao, J.; Guo, H.; Ha, S.; Joseph-McCarthy, D.; Kuchnir, L.; Kuczera, K.; Lau, F. T. K.; Mattos, C.; Michnick, S.; Ngo, T.; Nguyen, D. T.; Prodhom, B.; Reiher, W. E.; Roux, B.; Schlenkrich, M.; Smith, J. C.; Stote, R.; Straub, J.; Watanabe, M.; Wiorkiewicz-Kuczera, J.; Yin, D.; Karplus, M. *J. Phys. Chem. B* **1998**, *102*, 3586.
19. Sarkhel, S.; Sharon, A.; Trivedi, V.; Maulik, P. R.; Singh, M. M.; Venugopalan, P.; Ray, S. *Bioorg. Med. Chem.* **2003**, *11*, 5025.
20. Shao, D. L.; Berrodin, T. J.; Manas, E.; Hauze, D.; Powers, R.; Bapat, A.; Gonder, D. I.; Winneker, R. C.; Frail, D. E. *J. Steroid Biochem. Mol. Biol.* **2004**, *88*, 351.
21. Amari, G.; Armani, E.; Ghirardi, S.; Delcanale, M.; Civelli, M.; Caruso, P. L.; Galbiati, E.; Lipreri, M.;

Rivara, S.; Lodola, A.; Mor, M. *Bioorg. Med. Chem.* **2004**, *12*, 3763.
22. Wolohan, P.; Reichert, D. E. *J. Comput.-Aided Mol. Des.* **2003**, *17*, 313.
23. Coleman, K. P.; Toscano, W. A.; Wiese, T. E. *QSAR Comb. Sci.* **2003**, *22*, 78.
24. Sippl, W. *Bioorg. Med. Chem.* **2002**, *10*, 3741.
25. Kekenes-Huskey, P. M.; Vaidehi, N.; Floriano, W. B.; Goddard, W. A. *J. Phys. Chem. B* **2003**, *107*, 11549.
26. Vaidehi, N.; Floriano, W. B.; Trabanino, R.; Hall, S. E.; Freddolino, P.; Choi, E. J.; Zamanakos, G.; Goddard, W. A. *Proc. Natl. Acad. Sci. U.S.A.* **2002**, *99*, 12622.
27. Floriano, W. B.; Vaidehi, N.; Goddard, W. A.; Singer, M. S.; Shepherd, G. M. *Proc. Natl. Acad. Sci. U.S.A.* **2000**, *97*, 10712.
28. Schafer, J. M.; Liu, H.; Levenson, A. S.; Horiguchi, J.; Chen, Z. H.; Jordan, C. *J. Steroid Biochem. Mol. Biol.* **2001**, *78*, 41.
29. Ewing, T. J. A.; Makino, S.; Skillman, A. G.; Kuntz, I. D. *J. Comput.-Aided Mol. Des.* **2001**, *15*, 411.
30. Brooks, B. R.; Bruccoleri, R. E.; Olafson, B. D.; States, D. J.; Swaminathan, S.; Karplus, M. *J. Comput. Chem.* **1983**, *4*, 187.
31. Freist, W.; Sternbach, H.; Cramer, F. *Eur. J. Biochem.* **1996**, *240*, 526.
32. Gasteiger, J.; Marsili, M. *Tetrahedron Lett.* **1978**, 3181.
33. Rabenstein, B.; Ullmann, G. M.; Knapp, E. W. *Biochemistry* **2000**, *39*, 10487.
34. Connolly, M. L. *J. Appl. Crystallogr.* **1983**, *16*, 548.
35. Kuntz, I. D.; Blaney, J. M.; Oatley, S. J.; Langridge, R.; Ferrin, T. E. *J. Mol. Biol.* **1982**, *161*, 269.